gp.genomicpress.com

Genomic Psychiatry

OPEN

HIGH PRIORITY RESEARCH COMMUNICATION

Prepartum bumetanide treatment reverses altered neonatal social communication but nonspecifically reduces postpubertal social behavior in a mouse model of fragile X syndrome

Yui Sakamoto[1,#], Takeshi Takano[2,3,#], Shuji Shimoyama[4,#], Takeshi Hiramoto[2], Noboru Hiroi[2,5,6], and Kazuhiko Nakamura[1]

Fragile X syndrome is caused by monogenic silencing of the *FMR1* gene and is characterized by high rates of autism spectrum disorder. A previous study demonstrated that prepartum administration of bumetanide, a chloride transporter blocker, normalized neonatal vocalization in non-congenic *Fmr1* knockout (KO) pups. However, the genuine contribution of *Fmr1* deletion to this phenotype in a congenic *Fmr1* KO mouse model and the long-lasting effect of prepartum bumetanide administration on postpubertal social interaction remains unclear. The current study aimed to determine the impact of prepartum bumetanide administration on vocalization at postnatal day 7 and social interaction at 6 and 8 weeks of age in a congenic *Fmr1* KO mouse model in which the genetic backgrounds were homogeneous between KO and wild-type (WT) littermates. Moreover, we applied a computational analytical algorithm and determined predictive variables of neonatal vocalization for postpubertal social interaction. Our data showed that (1) KO mice exhibited altered numbers and sequences of distinct call types during neonatal vocalization and reduced social interaction at 6 weeks, (2) select sets of neonatal vocalization variables predicted postpubertal social interaction levels, and (3) bumetanide restored neonatal vocalization in KO pups but nonspecifically reduced social interaction in WT and KO mice at 6 weeks. These data indicate that *Fmr1* deletion selectively impacts distinct elements of neonatal vocalization and postpubertal social interaction. Additionally, bumetanide selectively restores neonatal vocalization but has a transient nonspecific negative impact on subsequent postpubertal social interaction.

Genomic Psychiatry January 2025;1(1):61–72; doi: https://doi.org/10.61373/gp024h.0094

Keywords: Fragile X, Fmr1, FMRP, critical period, GABA, social communication, social interaction, machine learning, predictors

Introduction

Precision medicine has not been utilized in psychiatry because the precise mechanistic targets of psychiatric disorders are not well established. Gene and genomic variants provide a reliable entry point for a mechanistic understanding of psychiatric disorders and mechanism-based therapeutic options (1).

Fragile X syndrome is a neurodevelopmental disorder caused by monogenic mutation and transcriptional silencing of the fragile X messenger ribonucleoprotein 1 (*FMR1*) gene, resulting in loss of its protein product, fragile X messenger ribonucleoprotein (FMRP). The syndrome includes the clinical diagnoses of autism spectrum disorder (ASD) and intellectual disability. Although *FMR1* silencing begins in the embryonic period in humans (2), the phenotypes are not reliably identified until later in the postnatal period, partly because clinical diagnoses are not feasible until formal tests can be reliably applied. However, many social, cognitive, affective, motor, and sensory phenotypes appear during early postnatal periods (3).

In the mouse brain, FMRP expression is high on embryonic day 11.5 (E11.5), E18.5, and during the first postnatal week but steadily declines thereafter (4, 5). The *Fmr1* peaks during the perinatal period mirror those in human brains (5). The developmental phase from the embryonic period to the first neonatal week, except for the time of birth (i.e., postnatal day 0, P0), is a unique period in which the inhibitory neurotransmitter gamma-aminobutyric acid (GABA) exerts an excitatory action on neurons because of their high intracellular chloride concentration (6, 7). Remarkably, a seminal study by Ben-Ari and colleagues reported that this transient inhibitory role of GABA at and near P0 is attenuated in a mouse model of fragile X syndrome; when pregnant mothers were treated with bumetanide, an NKCC1 chloride transporter inhibitor, one day before delivery, the increased probabilities of two neonatal call types (i.e., chevron and downward) were normalized in non-congenic *Fmr1* knockout (KO) pups at P8 (8). Human studies have not addressed the critical period for bumetanide treatment due to technical and ethical issues. The therapeutic effects of bumetanide on patients with idiopathic ASD are largely negative when treatment starts at 2 years of age or later (9).

The impetus of the present study was 3-fold. First, a non-congenic mouse model poses an interpretative issue. Although non-congenic mouse models have randomly shuffled allelic distributions throughout the genomes of KO and wild-type (WT) littermates, they have a systematic, consistent bias near the targeted gene. Because of the low recombination rates between the targeted gene and genes located nearby, the alleles of nearby genes of the targeted gene tend to be inherited together. Because gene targeting is induced in embryonic stem (ES) cells of the 129/Sv substrains and mice are bred with another strain (e.g., FVB or C57BL/6J), KO offspring accumulate alleles of neighboring genes derived from ES cells, and WT offspring accumulate alleles of breeders. Because these strains differ in their molecular, cellular, electrophysiological, anatomical, and behavioral phenotypes, any phenotypic differences between non-congenic KO and WT littermates cannot be unequivocally attributed to the targeted gene (10). We addressed this issue using a congenic *Fmr1* KO mouse model.

[1]Department of Neuropsychiatry, Hirosaki University Graduate School of Medicine, Hirosaki, Aomori, Japan 036-8562; [2]Department of Pharmacology, University of Texas Health Science Center at San Antonio, San Antonio, TX, USA 78229; [3]Tokyo Denki University, Ishizuka, Hatoyama-machi, Hiki-gun, Saitama 350-0394, Japan; [4]Department of Neurophysiology, Hirosaki University Graduate School of Medicine, Hirosaki, Aomori, Japan 036-8562; [5]Department of Cellular and Integrative Physiology, University of Texas Health Science Center at San Antonio, San Antonio, TX, USA 78229; [6]Department of Cell Systems Anatomy, University of Texas Health Science Center at San Antonio, San Antonio, TX, USA 78229

[#]These authors contributed equally to this work.

Corresponding Authors: Kazuhiko Nakamura, Hirosaki University Graduate School of Medicine, 5 Zaifu-cho, Hirosaki, Aomori, 036-8562, Japan. Phone: 81-172-39-5066; E-mail: nakakazu@hirosaki-u.ac.jp; and Noboru Hiroi, University of Texas Health Science Center at San Antonio, 7703 Floyd Curl Dr, San Antonio, TX78229, USA. Phone: 210-567-4169; E-mail: hiroi@uthscsa.edu

Received: 23 October 2024. Revised: 16 November 2024 and 4 December 2024. Accepted: 9 December 2024.
Published online: 24 December 2024.

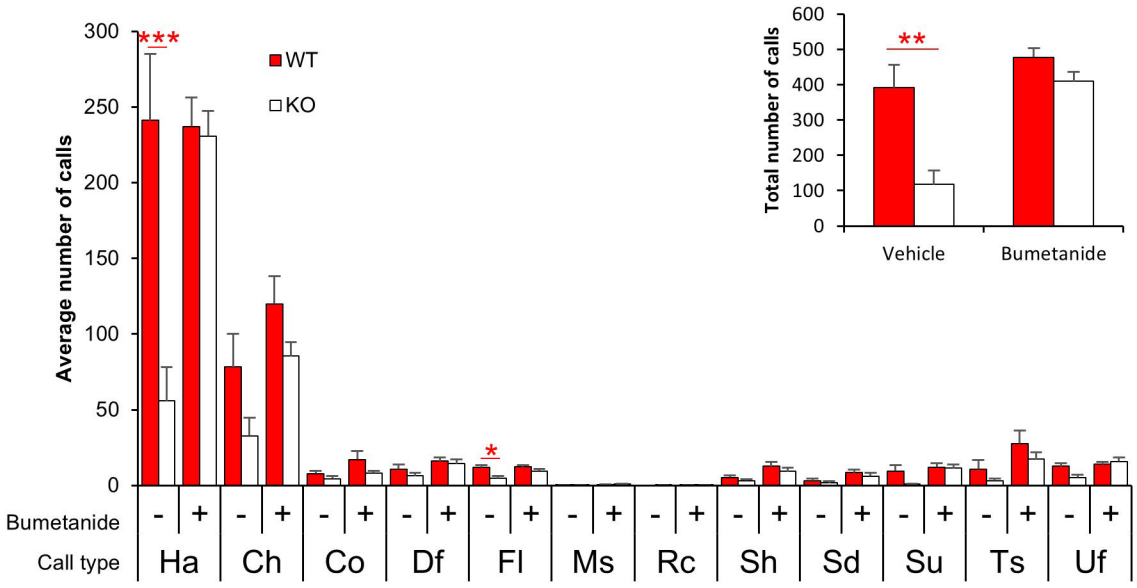

Figure 1. Number of neonatal vocalization call types. The average number (±SEM) of each call type emitted by male WT and KO mice is shown. Asterisks (*, **, and ***) indicate statistically significant differences (1%, 0.5%, and 0.1%, respectively) between WT and KO pups. Inset: WT and KO mice differed ($F(1,41) = 18.839$, $p < 0.0001$) and bumetanide increased calls in KO mice (Treatment, $F(1,41) = 23.080$, $p < 0.0001$; Interaction, $F(1,41) = 6.7576$, $p = 0.0129$). Student *t*-tests showed that WT and KO mice differed in the total number of all calls without bumetanide treatment ($p = 0.0013$), but not with bumetanide ($p = 0.0850$). Main figure: WT and KO mice differed depending on call types and treatment (Genotype x Call types x Treatment, $F(11,451) = 8.8573$, $p < 0.0001$). Vehicle-treated WT and KO pups differed in the numbers of harmonic ($p = 0.0007$) and flat ($p = 0.0072$). These significant differences of *t*-tests survived Benjamini–Hochberg's corrections for multiple comparisons at 5% FDR. Bumetanide-treated WT pups did not differ in any call type from bumetanide-treated KO pups ($p > 0.05$). Vehicle: WT, $n = 9$; KO, $n = 12$. Bumetanide: WT, $n = 12$; KO, $n = 12$. Ha, harmonic; Ch, chevron; Co, complex; Df, down-frequency modulation; Fl, flat; Ms, multi-step; Rc, reverse chevron; Sh, short; Sd, step-down; Su, step-up; Ts, two-step; Uf, up-frequency modulation.

Second, phenotypic variability is a norm, and thus comparisons based on group averages do not fully capture the nuanced nature of the impacts of genomic variations. *Fmr1* mutation does not cause complete penetrance, and approximately 60% of male carriers are diagnosed with ASD. Elements of ASD also show phenotypic variability; social communication is weak among *Fmr1* mutation carriers with an ASD diagnosis (3). More than 10 distinct call types and their specific temporal sequences are uniquely impacted by dose alterations of genes implicated in neurodevelopmental and psychiatric disorders in mouse models (11–13). Therefore, to capture the variable nature of this syndrome and its dimensional elements, we applied computational approaches (11, 12, 14, 15).

Third, specific roles of GABA during the perinatal period in the development of postpubertal social interaction have not been explored. This issue is pertinent to the theoretical question of whether normal neonatal social communication is a prerequisite for normal social interaction at later times or whether these two processes independently develop. We addressed this question by computationally evaluating the predictive power of variables of neonatal vocalization for postpubertal social interaction without and with bumetanide. Differential alteration of phenotypes of the two developmental stages by this treatment would support mechanistically independent processes; in contrast, the presence of predictive neonatal variables for postpubertal social interaction and improvement of both behaviors by bumetanide at the two developmental stages would be consistent with the hypothesis that the two developmental stages share a common mechanistic basis.

To test the hypothesis that a GABAergic tone during the perinatal period is a determinant for neonatal social communication and postpubertal social interaction, we administered bumetanide prepartum and evaluated its impacts on neonatal vocalization at P7 and on postpubertal social interaction at 6 and 8 weeks of age. As fragile X syndrome is associated with variable expressivity and developmental trajectories among carriers, we applied a computational analytical algorithm (12) to predict the variability of postpubertal social interaction scores from the variation in neonatal vocalizations.

Results

Fmr1 Deletion Alters the Number of Calls with Specific Geometric Shapes

Evidence indicates that the perinatal/neonatal period is critical for the development of social behavior (16), and neonatal vocalization is the earliest expression of social communication in rodents and humans (11, 12, 17, 18). It was reported that the probabilities of calls with two specific geometric shapes, termed chevron and downward, were increased and these increases were normalized by bumetanide in a non-congenic mouse model of fragile X syndrome (8). However, mouse pups generally exhibit more than 10 distinct call types, and they are distinctly impacted by genes linked to neurodevelopmental disorders (11–13, 19, 20). In particular, the call types that are altered in various mouse models of fragile X syndrome vary depending on genetic backgrounds, sex, age, call classifications, and other factors. When neonatal call types were analyzed in mouse models of fragile X syndrome in which the genetic backgrounds were made homogenous between WT and KO pups, various call types were found to be altered, resulting in greater numbers of "frequency jump" calls, which included two-syllable and frequency step calls, at P7 (13), increased percentages of chevron and frequency step call types and decreased percentages of complex, composite, downward, harmonic, two-syllable, and short call types at P8 (21).

We comprehensively characterized call types that were altered by *Fmr1* deletion and bumetanide treatment in congenic *Fmr1* KO pups and their WT littermates. KO pups emitted fewer total calls than WT pups, and this effect was ameliorated by bumetanide at P7 (Figure 1 inset). The numbers of the 12 call types were separately compared between WT and KO mice (Figure 1; Supplemental Table S2). Compared with WT pups, KO pups emitted fewer harmonic and flat call types. Bumetanide increased the number of calls in KO pups to the extent that KO and WT pups did not differ for any call types.

We additionally examined the proportion of each call type within the total number for each pup. In this measure, WT and KO mice did not differ for call types and bumetanide had no significant effect (Supplemental Figure S1; Supplemental Table S2).

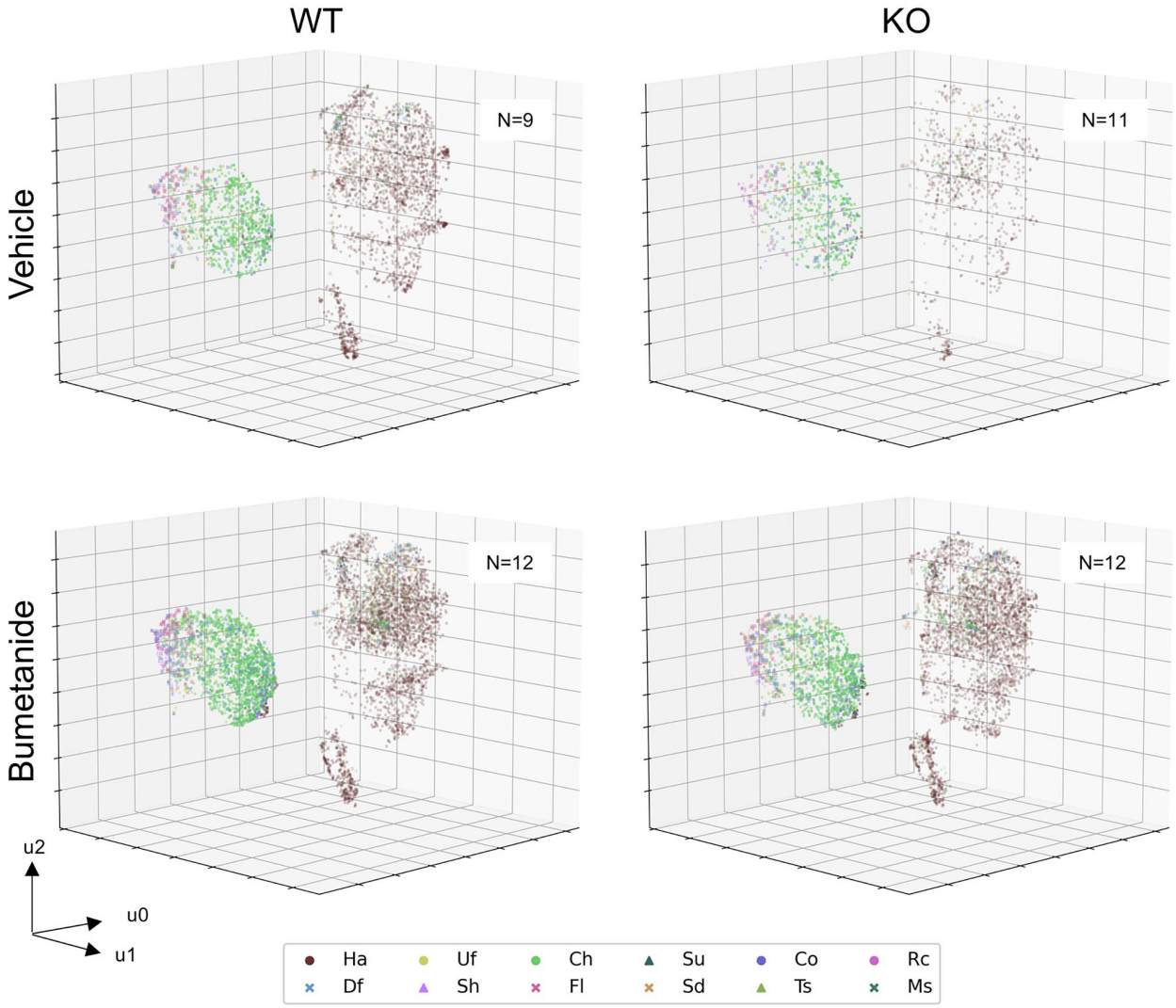

Figure 2. Three-dimensional UMAP of VocalMat parameters. UMAP was used to convert the quantitative acoustic parameters into lower dimensions while maintaining their character. The VocalMat parameters included "duration," "min_freq_main," "max_freq_main," "mean_freq_main," "bandwidth," "min_freq_total," "max_freq_total,""mean_freq_total," "min_intens_total," "max_intens_total," and "mean_intens_total". Calls were separated into three clusters. Call types are indicated by distinct colors in the three clusters.

The length of all calls (Supplemental Figure S2 inset) or each call type (Supplemental Figure S2) did not differ between WT and KO pups. While the lengths of all calls were prolonged by bumetanide (Figure 2 inset), they did not reach significance when each call was separately analyzed (Supplemental Figure S2).

Fmr1 Deletion does not Alter the Quantitative Acoustic Parameters of Call Types

These analyses were based on the categorical classification of geometric call shapes. However, each call type also has quantitative acoustic parameters. We thus additionally analyzed the (1) bandwidth in Hz, (2) maximum, mean, and minimum frequencies in Hz of a call or its main components, and (3) maximum, mean, and minimum intensities of each call. Vehicle-treated WT and KO pups did not differ in any of these acoustic parameters for all call types (Supplemental Table S3A–S3J). Thus, the acoustic parameters did not discriminate genotype.

Fmr1 Deletion Impacts the Quantitative Parameters of Calls in a Dimensional Space

Having established that the simple acoustic parameters did not differentiate genotype or drug treatment, we next aimed to evaluate calls in an independent dimension. We visualized and evaluated the complex nature of VocalMat's quantitative acoustic parameters in three and two dimensions using Uniform Manifold Approximation and Projection (UMAP).

We first used three commonly used UMAP metrics: Manhattan, Euclidean, and Chebyshev (Supplemental Figure S3). To evaluate the relationship between these UMAP clusters and call types, we color-coded each data point based on the call classification of our modified VocalMat. Because the Euclidean metrics provided better cluster separation than the Manhattan or Chebyshev metrics, we used the Euclidean metric for all the subsequent analyses.

This analysis reduced all calls into three main spatial clusters in a three-dimensional UMAP space (Figure 2; Supplemental Figures S4 and S5). The decreased numbers of calls are apparent in all three clusters in KO pups; all these spatial clusters were restored by bumetanide. Harmonic calls were predominantly represented in spatial Cluster 1 and Cluster 3 (Supplemental Figures S5 and S6); chevron was the most predominant call type in Cluster 2 (Supplemental Figures S5 and S6). This analysis showed quantitative differences and similarities among VocalMat-based call types. Calls classified as "harmonic" have the most variable quantitative profile than other call types.

The combined analytical approaches for categorical call types and quantitative acoustic parameters showed that *Fmr1* deletion and

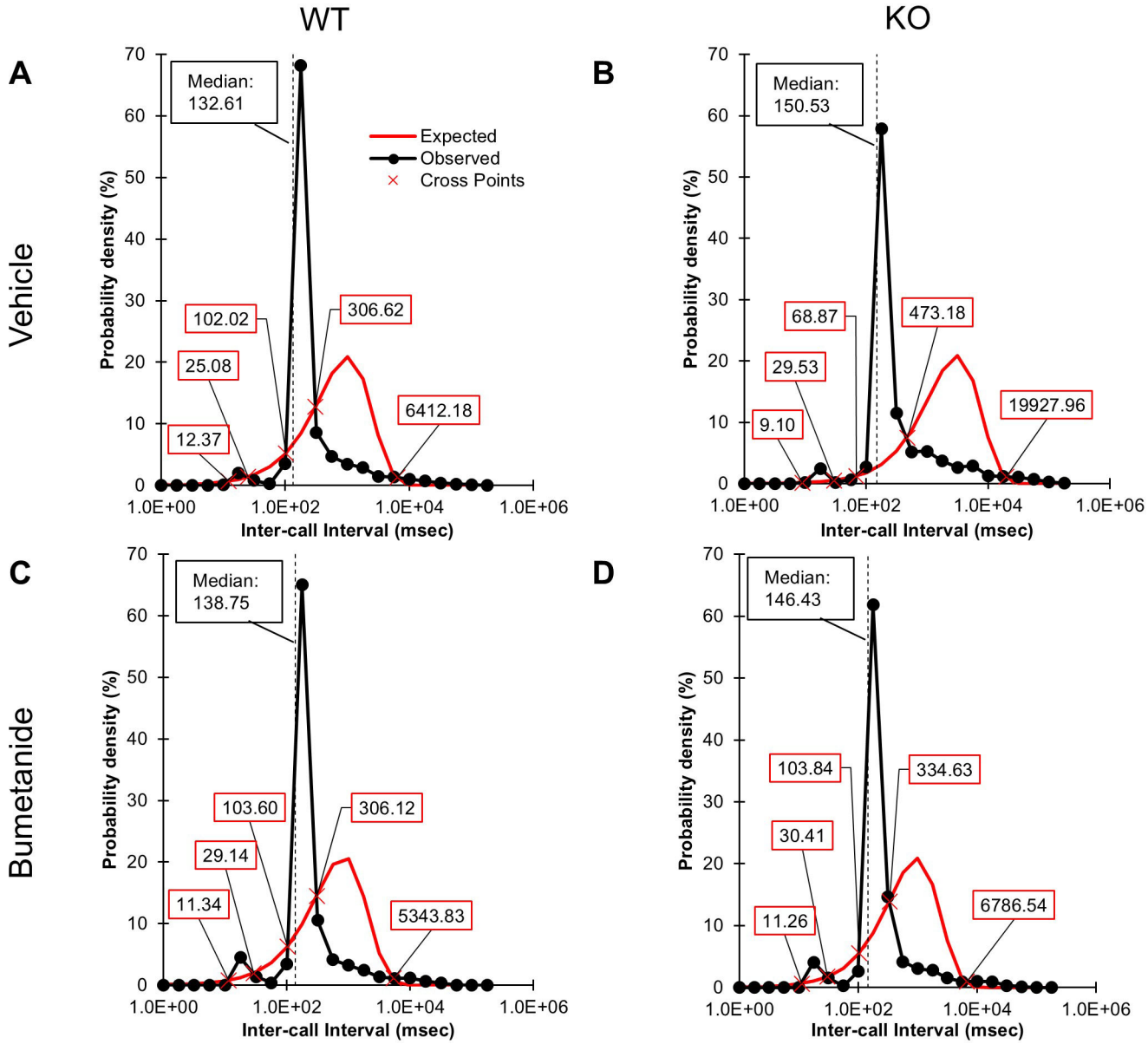

Figure 3. Probabilities of intercall intervals. The observed and expected probabilities of intercall intervals of vehicle-treated WT (**A**), vehicle-treated KO (**B**), bumetanide-treated WT (**C**), and bumetanide-treated KO mice (**D**). Vehicle-treated KO pups had longer intercall intervals, compared with vehicle-treated WT pups ($p < 0.0001$). Bumetanide reduced intercall intervals in KO pups ($p < 0.0001$) but bumetanide-treated KO pups still maintained longer intercall intervals than bumetanide-treated WT pups ($p < 0.0001$). The actual intercall intervals (ms) at cross-points of the observed and expected probabilities are shown. Intercall intervals shorter than the higher cross-points between the observed and expected distributions had probabilities higher than the expected distributions and thus are considered intervals between calls within sequences (Vehicle-WT, 306.62 ms; Vehicle-KO, 473.18 ms; Bumetanide-WT, 306.12 ms; Bumetanide-KO, 334.63 ms); intercall intervals longer than the cross-points were considered intervals from the end of a sequence to the beginning of the next sequence.

bumetanide impact calls with distinct categorical and quantitative parameters.

Fmr1 KO Alters the Temporal Distribution of Call Sequences

Calls were emitted with various intercall intervals. To objectively identify a temporal cluster of calls, we first determined the Poisson distribution, a theoretically expected distribution of intercall intervals with a given number of calls within a 300-s test time (Figure 3, red lines). Because KO pups emitted fewer calls than WT pups, the theoretically expected intercall intervals of KO pups were shifted to the right (Figure 3B, red lines) compared with those of WT pups (Figure 3A, red lines). These data indicate that *Fmr1* deletion alters the intercall intervals without changing the length of each call (see Supplemental Figure S2).

The largest peaks of observed intercall intervals, representing the most frequent intercall intervals, were found around 200 ms (Figure 3, black lines). There were also much smaller peaks that occurred more frequently than expected from the Poisson distributions below approximately 30 ms (Figure 3, black lines). However, these short intercall intervals occurred in less than 5% of all calls of all pups.

We defined a call sequence as a series of calls that were emitted with intercall intervals shorter than the larger value of the two crosses between the highest probability peak of the observed curve and the expected probability curve (see Figure 3A, WT, Vehicle, 306.62 ms; B, KO, Vehicle, 473.18 ms; C, WT, Bumetanide, 306.12 ms; D, KO, Bumetanide, 334.63 ms).

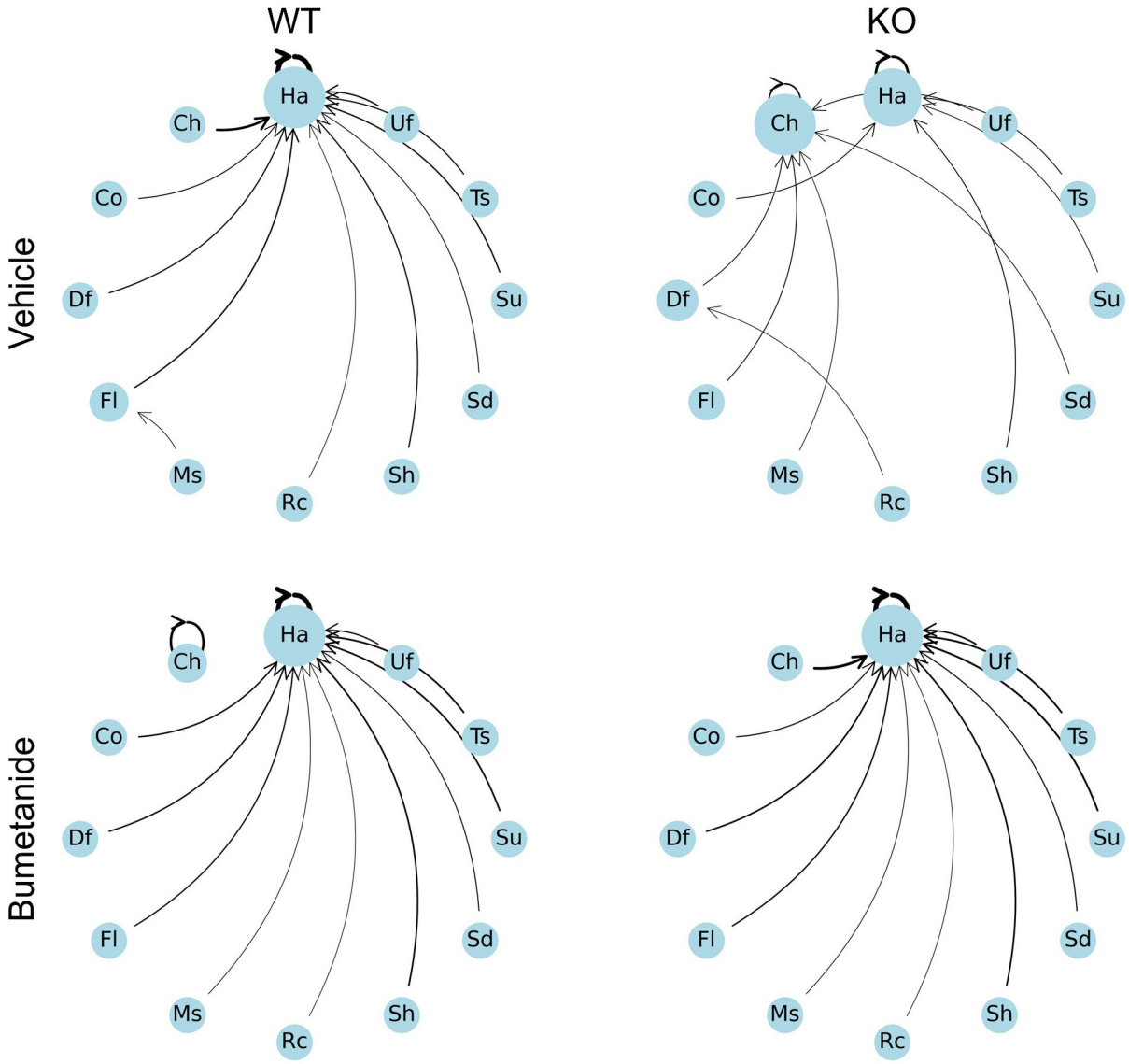

Figure 4. Markov model. The relative probabilities of each two-call sequence for each of the 12 call types identified by the Markov models are shown. The sum of all proportions of each starting call is 1, and the sum of all Markov probabilities is 100% × 12 calls. The line thickness represents the relative probability of a call sequence.

When call sequences were so defined, short and long sequences were identified around 100 ms and 1 s, respectively (Supplemental Figure S7). Bumetanide lengthened the long sequence duration in KO pups compared with that in vehicle-treated KO pups.

Fmr1 KO Alters Call Sequences

Having defined call sequences, we next determined how various call types were ordered within sequences. We determined the probabilities of two consecutive calls for a given starting call using Markov modeling. This model is based on the Markov property, where future states depend only on the current state. The probabilities of call sequences were determined based on two consecutive calls. In other words, the probability of the next call type was computed within each call type; the sum of probabilities of all two-call sequences starting from a given call type was always 1.0. Thus, this analysis was not influenced by the probabilities of the first call of two consecutive calls emitted by each subject. This analysis revealed distinct frequently emitted two consecutive calls of vehicle-treated WT and KO pups (Figure 4). Bumetanide restored the altered two-call sequences of KO pups.

Because of the Markov property, the two-call sequences starting from less emitted call types tend to be overestimated. To evaluate call sequences within each mouse with all starting call types, we incorporated a separate analysis of how frequently each two-call pair was emitted. In this analysis, the sum of probabilities of all two-call sequences starting from all call types was always 1.0. Two-call pairs starting and ending in harmonic were predominant in all groups (Supplemental Figure S8).

Prepartum Bumetanide Treatment Reduces Postpubertal Social Interaction in KO Mice

When the pups reached 6 and 8 weeks of age, they were sequentially tested for social interaction. We tested naturalistic social interaction in a home cage setting because it is a better validation than other procedures (22), and molecular mechanisms underlying direct social contact in such a set-up and indirect contact with a barrier differ (23).

There were a few test or stimulus partner mice in each group that exhibited aggressive behavior. Such cases were eliminated from the analysis (24) for three reasons. First, genetic bases of affiliative social interaction and aggressive behavior are nonidentical (25). Second, aggressive

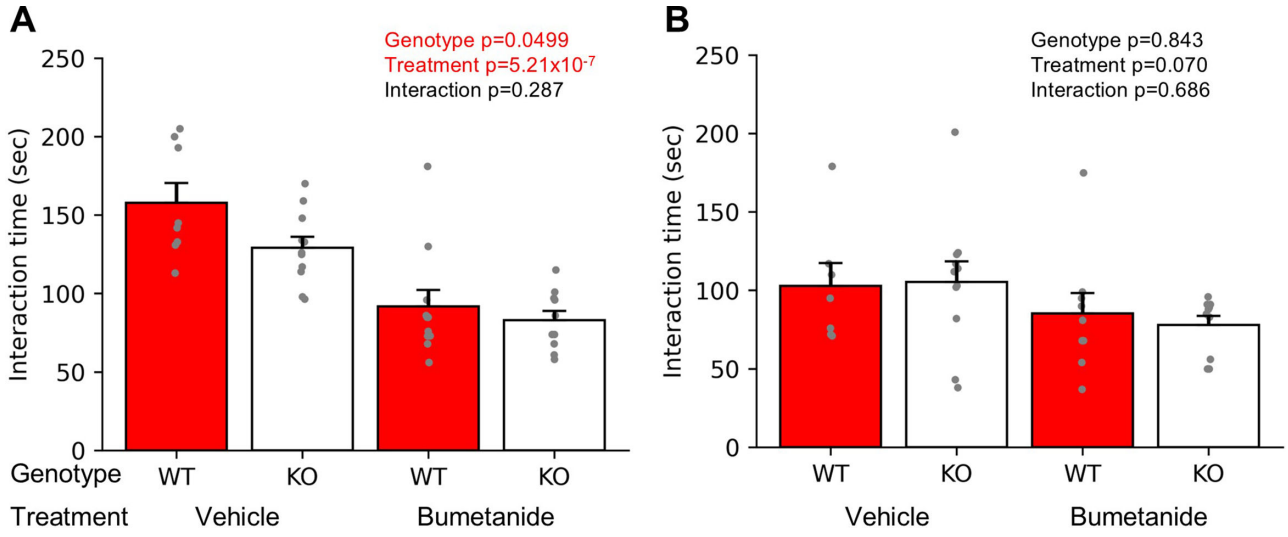

Figure 5. Social interaction. The time (mean±SEM) spent in active social interaction at 6 weeks of age (**A**) and 8 weeks of age (**B**) is shown. (**A**) KO mice spent less time in social interaction than WT mice (Genotype, $F(1,36) = 4.1160$, $p = 0.0499$) and bumetanide treatment equally reduced social interaction in both genotype groups (Treatment, $F(1,36) = 37.1341$, $p < 0.0001$; Interaction, $F(1,36) = 1.1674$, $p = 0.2871$). WT/Vehicle, $n = 8$; KO/Vehicle, $n = 11$; WT/Bumetanide, $n = 11$, KO/Bumetanide, $n = 10$. (**B**) WT and KO mice did not differ (Genotype, $F(1, 33) = 0.0399$, $p = 0.8429$) and the effect of bumetanide treatment was not significant ($F(1,33) = 3.4975$, $p = 0.0704$) without an interaction effect ($F(1,33) = 0.1661$, $p = 0.6862$). WT/Vehicle, $n = 7$; KO/Vehicle, $n = 11$; WT/Bumetanide, $n = 9$, KO/Bumetanide, $n = 10$.

behavior is not a prominent element of fragile X syndrome, but altered affiliative social interaction is an element. Third, aggressive behavior indirectly suppresses the occurrence of affiliative social interaction, thereby artificially underestimating it. The following test mice were eliminated in each group: 6 weeks: Vehicle WT, 1 mouse; Bumetanide WT, 1 mouse; Bumetanide KO, 2 mice. 8 weeks: Vehicle WT, 1 mouse; Bumetanide WT, 3 mice; Bumetanide KO, 1 mouse. We also eliminated cases where the stimulus mice were agitated and hyperactive (6 weeks, Vehicle KO, 1 case. 8 weeks: Vehicle WT, 1 case; Bumetanide KO, 1 case), as such behavior of the stimulus mouse makes it physically impossible for a test mouse to engage in affiliative social interaction.

KO mice showed lower social interaction levels than WT mice; prepartum bumetanide treatment equally lowered social interaction levels in both WT and KO mice at 6 weeks of age (Figure 5A).

At 8 weeks of age, vehicle-treated WT and KO mice did not differ, and bumetanide had no statistically significant effect on social interaction in WT and KO mice (Figure 5B).

Predictive Variables of Neonatal Vocalization for Postpubertal Affiliative Social Interaction

If a mechanistic link exists between neonatal vocalizations and the development of postpubertal social behavior, the former should predict the latter. To identify such predictive variables of neonatal vocalizations among the numbers and probabilities of call types and call sequences, we developed Least Absolute Shrinkage and Selection Operator (Lasso) regression models for each group. The acoustic variables were not included in this analysis, as there was no difference in their averages between genotypes or treatments, and some call types were not emitted in some mice, thus providing no acoustic parameter (e.g., bandwidth and amplitude) (Supplemental Table S3).

This analysis identified a unique set of specific variables within each group that predict affiliative social interaction levels at 6 weeks of age (Figure 6). The most robust predictors of vehicle-treated WT mice were the number of flat->chevron and the proportion of chevron->chevron; those of vehicle-treated KO mice were the Markov probability of chevron->short, and the non-Markov proportions of harmonic->chevron and chevron->two-step calls. These variables were also significantly correlated with the scores of social interaction (see Figure 6 inset; Supplemental Table S2; Supplemental Figure S6).

In bumetanide-treated mice, several variables of neonatal vocalization were identified as predictors by Lasso models (Figure 6). The most robust predictors were the proportion of two steps->flat and Markov probability of harmonic->step-up in WT mice; the Markov probabilities of step-down->harmonic, harmonic->chevron, complex->upward frequency modulation, and chevron->two steps, and non-Markov proportions of downward frequency modulation->flat in KO mice. Remarkably, none of the Lasso-selected variables were significantly correlated with social interaction scores in bumetanide-treated WT or KO mice (Figure 6 inset; Supplemental Table S2; Supplemental Figure S6). This result is likely due to the nonspecific effects of bumetanide on social interaction in both WT and KO mice (see Figure 5).

In the analysis above, we identified neonatal call parameters that best predicted postpubertal social interaction within 6-week vehicle-treated WT or KO mice. We next identified neonatal call parameters that best differentiated social interaction scores and genotypes in pooled data of both vehicle-treated WT and KO mice at 6 weeks. First, a Lasso regression model with social scores as the coefficient identified sequences and call numbers as predictors of social interaction (Supplemental Figure S9A, e.g., Fl->Ch, Sh->Fl). Only two of them were significantly correlated with social interaction scores (Fl->Ch and Ch->Sh; Supplemental Table S2; Supplemental Figure S9A). Second, a Lasso regression model identified the number of Flat->Chevron as a predictor of the genotype (Supplemental Figure S9B). However, this predictor failed to discriminate the genotype (see Supplemental Figure S9B and Supplemental Table S2).

Although there was no effect of genotype or bumetanide on social interaction at 8 weeks of age (Figure 5), we applied the Lasso method to determine which neonatal vocalization variables predict individual variation in social interaction (Supplemental Figure S10). Distinct sets of two-call sequences predicted individual variation within each genotype, including the Markov probability of complex->chevron and the non-Markov proportion of chevron->complex in vehicle-treated WT mice. In vehicle-treated KO mice, the Markov probability of upward frequency modulation->two steps and the non-Markov proportion of harmonic->chevron were robust predictors.

In bumetanide-treated WT mice, Lasso models identified some sequences (e.g., complex->upward frequency modulation and two-step->upward frequency modulation; Supplemental Figure S10), all of which

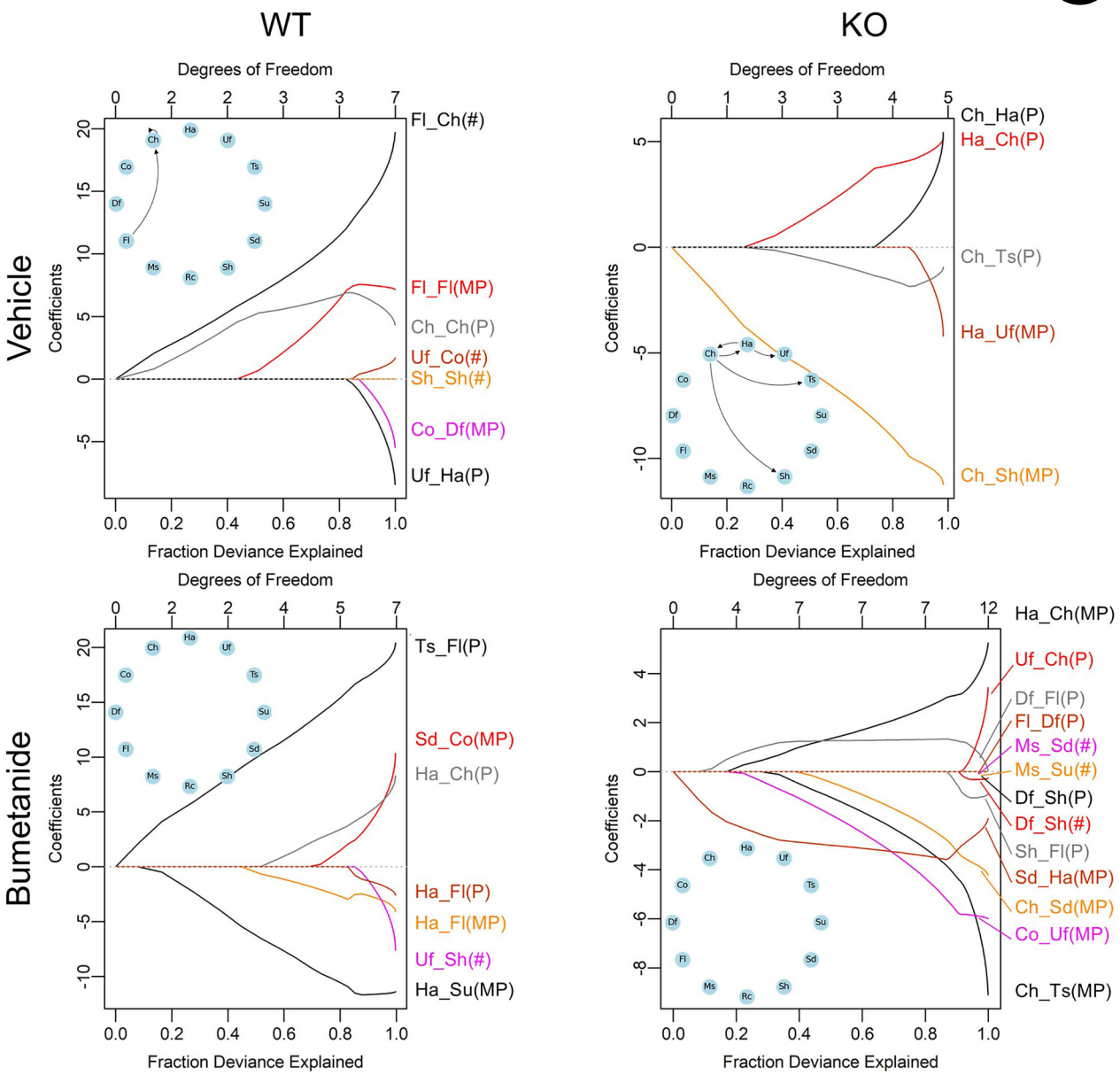

Figure 6. Neonatal vocalization predictors for social interaction at 6 weeks of age. The fraction of deviance explained and the coefficients of variables were determined by the Lasso regression model. All parameters (call type number and proportions, call sequence number, Markov probabilities, and non-Markov proportions) were used for selection. Lasso models identified several predictors for social interaction scores within each group. Each inset shows call sequences that were significantly correlated with the individual post-pubertal social interaction scores (see Supplemental Table S2 and Figure 6). The Markov probabilities, non-Markov proportions, and numbers of two-call sequences were selected. The small values along the fraction of deviance explained axis are robust predictors of social interaction. Ha, harmonic; Ch, chevron; Co, complex; Df, down-frequency modulation; Fl, flat; Ms, multi-step; Rc, reverse chevron; Sh, short; Sd, step-down; Su, step-up; Ts, two-step; Uf, up-frequency modulation, MP, Markov probability; P, non-Markov proportion; #, number.

were significantly correlated with the postpubertal social interaction scores (Supplemental Figure S10 inset; Supplemental Table S2).

In bumetanide-treated KO mice, a Lasso model selected the Markov probability of flat->upward frequency modulation and upward frequency modulation->upward frequency modulation and number of short->short as the most robust predictors for social interaction (Supplemental Figure S10), none of which were significantly correlated with the social scores (Supplemental Figure S10 inset; Supplemental Table S2).

Discussion

We hypothesized that the intracellular concentration of chloride ions in neurons around the time of birth is a critical determinant for the causal sequential development of neonatal and postpubertal social behaviors. This hypothesis was based on the pioneering report that bumetanide, an NKCC1 (Na^+-K^+-$2Cl^-$ cotransporter) inhibitor that controls intracellular chloride ion concentration, restored neonatal vocalizations in non-congenic *Fmr1* KO pups (8). We used a congenic *Fmr1* KO mouse to determine the predictive variables of neonatal vocalization for the post-pubertal social interaction scores as well as the impact of bumetanide on these developmental variables. Our data showed that (1) *Fmr1* deletion reduced the number of specific neonatal call types and probabilities of call sequences; (2) bumetanide restored these neonatal phenotypes; (3) *Fmr1* deletion reduced direct social interaction at 6 weeks, but not at 8 weeks, of age; (4) bumetanide nonspecifically reduced the postpubertal social interaction level in WT and KO mice, resulting in indistinguishable

social interaction levels at 6 weeks; (5) distinct neonatal vocalization call sequences predicted the postpubertal social interaction level in vehicle-treated WT and KO mice at 6 weeks; and (6) such predictors did not exist in bumetanide-treated WT and KO mice because bumetanide nonspecifically reduced social interaction scores to the level where the two genotype groups were indistinguishable.

Unless unavoidable, we will discuss only those studies that used congenic or coisogenic *Fmr1* KO mice lines or an F1 hybrid line where the homogeneous genetic backgrounds of WT and KO mice are maintained. Non-congenic mice with "mixed" genetic backgrounds consistently carry more breeder line alleles in WT mice and more ES cell alleles (e.g., 129/Sv) in KO mice near the deleted gene (10). Such models do not identify phenotypes that genuinely reflect the impact of *Fmr1* deletion alone. Moreover, we limit our discussion to studies that manually classified calls or used automatic call classification systems with low false negative and false positive rates because high false negative and positive rates compromise the accurate evaluation of neonatal calls (26).

We observed that male congenic *Fmr1* KO mice emitted fewer calls of specific call types (harmonic and flat) but exhibited normal percentages of all call types. Previous well-controlled studies identified alterations of various neonatal vocalization parameters in congenic *Fmr1* KO pups. Congenic *Fmr1* KO pups with an FVB background emitted more two-syllable and frequency steps at P7 than WT pups; however, sex was not specified in this study (13). In another study, male congenic *Fmr1* KO pups with an FVB background emitted fewer calls at P9 and P13 and more calls at P12 than WT pups (27). Our results are consistent with this observation in that KO pups emitted fewer calls than WT pups (see Figure 1 inset). While power analyses indicate that statistically significant differences might be achieved with larger sample sizes for chevron ($n = 22$), step-up ($N = 13$), up-frequency modulation ($N = 15$), all the other call types are estimated to require much large sample sizes (see Supplemental Table S2 and Figure 1, Power analysis). Thus, *Fmr1* KO affects harmonic and flat call types more robustly than other calls.

When calls were analyzed by proportions, we found decreased proportions of harmonic and two-step calls and higher proportions of chevron in KO pups. However, none of these alterations reached statistical significance. In a previous study, male *Fmr1* KO pups with an FVB background produced proportionally more chevron and frequency step call types and decreased proportions of complex, composite, downward, harmonic, two-syllable, and short call types at P8 (21). A larger sample size of their study (WT, $n = 17$; KO, $n = 13$) is one likely factor for significance in more call types in their study than in our study (WT, $n = 9$; KO, $n = 12$). Power analyses showed that with larger sample sizes, vehicle-treated WT and KO mice are likely to achieve a statistically significant reduction in proportions of harmonic ($N = 13$) and step-up (similar to two-syllable, $N = 45$) calls and increases in down-frequency modulation (similar to downward) ($N = 39$) and short ($N = 48$) calls (Supplemental Table S2; Supplemental Figure S1). The other call types require much larger sample sizes to achieve statistical significance: chevron ($N = 69$), frequency step (multiple steps, $N = 830$; two steps, $N = 704$), complex ($N = 638$) call types (Supplemental Table S2; Supplemental Figure S1). Together with these power analyses, our data clearly indicate that *Fmr1* deletion impacts the proportions of harmonic, down-frequency modulation, step-up, and short calls in this order.

A previous study demonstrated that non-congenic *Fmr1* KO mice exhibited *higher* probabilities of chevron and downward call types than WT pups at P8 (8). Our study showed that the percentages of chevron and down-frequency modulation calls were higher in male KO pups than in male WT pups at P7 (Supplemental Figure S1), and bumetanide tended to correct these trends when using sample sizes ($n = 9$–12) similar to those in the previous study (8) ($n = 9$–13). However, none of these trends achieved statistical significance in our study, although a power analysis indicates that an increased proportion of down-frequency modulation ($N = 39$) and chevron ($N = 69$) calls in KO mice may achieve significance with much larger sample sizes (see Supplemental Table S2 and Supplemental Figure S1). Several factors are likely. First, the study by Tyzio and colleagues eliminated pups that emitted less than 50 calls during a 3-min period, but we did not eliminate such cases because we considered low call numbers as a phenotype. Second, our and their recording time durations were 5 min and 3 min, respectively. The phenotype they detected might occur in the first 3 min of our testing. However, this was not the case; when data of the first 3 min were analyzed, we still did not find statistically significant increases in chevron or downward frequency modulation (Supplemental Table S2, Figure 1_Number_3 min; Supplemental Table S2, Figure 1_Proportion_3 min). Third, the study by Tyzio and colleagues did not determine the sex of mice used, whereas our study used males only. Fourth, their study analyzed and presented only chevron and downward call types. Despite these methodological differences, our data are consistent with their finding that *Fmr1* deletion alters the proportions of specific neonatal call types, and the effect is normalized by bumetanide. Our study further showed that bumetanide restored defective call sequences of KO pups to levels similar to those of WT pups. While a larger sample size might identify more call types that differ between the genotypes, it is clear that some call types (e.g., harmonic call types) are more easily affected by *Fmr1* deletion than others.

Our observations further extended the study of Tyzio and colleagues by including an analysis of postpubertal social interaction and the effects of bumetanide on this phenotype. *Fmr1* deletion impaired postpubertal direct social interaction at 6 but not 8 weeks of age. Previous studies of *Fmr1* KO mice did not consistently find robust social interaction deficits. Congenic *Fmr1* KO mice showed higher, indistinguishable, or lower levels of active direct social interaction than those of WT mice (28–34). These studies used 8- to 24-week-old mice. Our and others' data from 8-week-old mice indicate that *Fmr1* deletion has little or no effect on social approach and sociability at this age (32–34). Our observations suggest that detectable deficits in affiliative social interaction appear at 6 weeks of age. Moreover, we detected a statistically significant genotype difference after excluding cases where either stimulus or test mice exhibited aggressive behaviors or hyperactivity (see *Results*). It might be difficult to detect a subtle difference in affiliative social interaction in *Fmr1* KO mice if such confounding factors are not eliminated or not detectable in a three-chamber apparatus where aggressive and affiliative social approach cannot be separated and are equally recorded as more time in the vicinity of a caged stimulus mouse. In general, the rather weak defects in social behavior on a group basis in *Fmr1* KO mice are congruent with clinical observations that individuals with *Fmr1* deletions show incomplete penetrance for the full criteria of ASD diagnosis (35).

A novel aspect of the present study is that we identified neonatal vocalization sequences that best predict postpubertal social interaction scores. The number of flat->chevron and Markov probability of chevron->short sequence were significantly correlated with the postpubertal social interaction scores in a pooled data of vehicle-treated WT and KO mice (Supplemental Figure S9A). These parameters were also identified as the most robust predictors when the best predictors were explored within each genotype (see Figure 6). In other words, the level of these call sequences can provide insights into the future developmental trajectory of social interaction. This observation is not inconsistent with the hypothesis that a common developmental mechanism exists between neonatal social communication and postpubertal social interaction and that the normal postpubertal social interaction requires normal neonatal social communication, including the number of flat->chevron sequence. While the biological significance of these call sequences is not clear, we previously demonstrated that altered call sequences in a mouse mutant for another gene implicated in neurodevelopmental disorders lost the capacity to elicit maternal approach (11). More work is needed to critically evaluate whether the call sequence alteration of *Fmr1* KO pups contributes to a causal chain from the genotype of pups, impaired maternal care, and impaired development of social and cognitive capacities (17, 18).

While the number of flat->chevron was identified by a Lasso model as a predictor for the genotype (Supplemental Figure S9B), this variable did not clearly discriminate WT and KO genotypes (see Supplemental Table S2 and Supplemental Figure S9B). This weak discriminating power of the Lasso-identified variable is likely due to the overlapping nature of social interaction scores between WT and KO mice and a very weak difference in social scores between the two genotypes (Figure 5A). In more general

terms, the neonatal variables might be more suitable in predicting the continuous nature of postpubertal social scores than the categorical classification of the genotype.

Although the Lasso models extracted predictive neonatal call variables for the social interaction scores of each genotype with bumetanide treatment, no models achieved statistically significant correlation coefficients with the social interaction scores in bumetanide-treated WT and KO mice (Figure 6). One reason for the lack of correlations is that bumetanide treatment eliminated the effects of genotype on postpubertal social interaction by nonspecifically reducing the social interaction levels in WT and KO mice (see Figure 5). Thus, the effects of bumetanide on neonatal and postpubertal social behaviors are dissociated; bumetanide restored neonatal social communication but had nonspecific negative effects on postpubertal social interaction in WT and KO mice. This dissociation could be interpreted as suggesting that distinct mechanisms exist for neonatal social communication and postpubertal social interaction. More work is needed to critically evaluate the mechanistic origins of neonatal social communication and postpubertal social interaction.

This result does not support the hypothesis that bumetanide, when given around the time of birth, has beneficial effects on postpubertal social impairments in patients with fragile X syndrome. However, possibilities remain that lower doses of bumetanide have more specific ameliorative effects on the later social interaction or that this drug has beneficial effects on other types of social behavior such as social incentive learning (36) or maternal social behavior (11, 37) or nonsocial behaviors, including sensory hypersensitivity (38) and their cellular correlates (38, 39). Alternatively, distinct mechanistic origins and differential dependence on peripartum GABA signaling might exist for neonatal social communication and postpubertal social interaction. More work is needed to explore the possible effects of bumetanide administered at postnatal or earlier embryonic periods.

Although bumetanide is largely ineffective in alleviating ASD symptoms in humans, this treatment is generally started after a diagnosis of ASD at 2–3 years of age. If the perinatal period is the critical period for the therapeutic effects of bumetanide on neonatal social communication, as suggested by our observations, its therapeutic effects would be expected to be most robust when it is applied perinatally and its outcome is evaluated much earlier. Our observations and computational approaches provide a template for future work to explore the causally distinct neuronal substrates that subserve neonatal and later ASD-linked behaviors.

Methods

Mice

We used male FVB.129P2-Pde6^{+} Tyr $^{c\text{-}ch}$*Fmr1*^{tm1Cgr}/J mice (*Fmr1*$^{-/y}$, #004624, Jackson Laboratory, Bar Harbor, ME, USA) and their WT littermates. We chose male mice, as the symptoms of Fragile X syndrome in humans are more severe in males than females and female patients tend to exhibit a greater degree of interindividual variability (40). These mice were generated by crossing male *Fmr1*$^{-/y}$ mice (12–24 weeks old) with female *Fmr1*$^{+/-}$ mice (8–20 weeks old) as breeders. Their genotypes were determined by PCR using the following primers: 5′-TGTGATA GAATATGCAGCATGTGA-3′, WT forward; 5′-CACGAGACTAGTGAGACGTG-3′, homozygous forward; 5′-CTTCTGGCACCTCCAGCTT-3′, reverse for both genotypes.

This *Fmr1* mutant strain originally contained 129P2/OlaHsd alleles derived from E14 ES cells, but was converted to a congenic line through 11 generations of backcrossing of mutant mice to the FVB strain. This backcrossing eliminated both copies of the *Pde6b* mutant allele, a gene responsible for retinal degeneration; mutant mice do not suffer from retinal degeneration or blindness. Because this is a congenic strain, the confounding effects of unequally enriched 129P2/OlaHsd alleles surrounding the *Fmr1* gene in mutants and those of FVB alleles in their WT littermates are minimized (10).

Treatment

Female breeders were examined for a plug every day; when it was present, this was defined as 0.5 days post coitum (dpc). Pregnant females were then separated from their male partners. In the last week of pregnancy, cage bedding was not changed to minimize stress. Mice were randomly assigned to either the vehicle or bumetanide treatment group. At 18.5 dpc, bumetanide (#14630, Cayman Chemical Company, Ann Arbor, MI, USA) or vehicle was given in the drinking water, based on the expected volume consumption and the dam's body weight. This timepoint was chosen based on a published study (8). Our pilot study showed that mice consume at least 5 ml in 24 h, and the solution concentration was adjusted, based on the dam's weight, to greater than 2 mg/kg bumetanide. This regimen achieved the target dose when partum was confirmed at and after 19.5 dpc. The consumed dose of bumetanide ranged from 2.928 to 4.12 mg/kg (Supplemental Table S1).

Behavior

Male congenic *Fmr1*$^{+/y}$ (WT) and *Fmr1*$^{-/y}$ (KO) mice were used for behavioral analyses.

Ultrasonic Vocalization

When male pups reached P7, the cage containing the mother and the litter was transferred to the test room 30 min before testing. This developmental timepoint was chosen, as a previous study showed that *Fmr1* KO pups differed from WT pups in vocalizations at P7, but not at P4 or P10 (13). Moreover, another study tested the effects of bumetanide on vocalizations at P8 (8). Each pup was then moved to a test chamber (18 cm long × 18 cm wide × 30 cm high). Ultrasonic vocalizations were recorded for 5 min using an UltraSoundGate (Avisoft, Germany) connected to a computer equipped with Avisoft-RECORDER software (Avisoft). The sampling rate was set to 250 kHz (format, 16 bit). The low cut-off frequency was set at 10 kHz to reduce background noise outside the relevant frequency band. The frequency window for analysis ranged from 15 to 150 kHz. Call detection was performed using an automatic threshold-based algorithm and a hold time mechanism (hold time: 10 ms).

The weights of dams were measured to calculate the total dose of bumetanide they consumed. However, we did not measure the body weights of pups. The pups' body weights are not altered in this specific mouse model of fragile X syndrome (Jax#004624) compared with those of WT littermates, and no correlation of body weights with changes in call types was reported (41, 42).

Affiliative Social Interaction

Male mice that were tested for neonatal vocalization were sequentially tested for social interaction at 6 and 8 weeks of age. The test subjects and age-matched male *Fmr1*$^{+/y}$ non-littermates, used as stimulus mice, were habituated to the test room for 30 min. The test and stimulus mice were simultaneously placed in a test apparatus (20 cm long × 28 cm wide × 15 cm high; 50 lux), and their behavior was recorded for 5 min. Under this experimental condition, mice generally exhibit low levels of aggressive behaviors (12, 43–47). We used this naturalistic test instead of the three-chamber sociability test apparatus because the former is recommended for ultimate validation and the latter has many technical and interpretive issues (22, 48). Raters were blinded to the genotype and treatment until testing and scoring were completed.

Computational Analysis

Call Type Classification. Sonograms were inspected, and genuine noises were eliminated from the analysis. VocalMat software (26) was used to determine call types. This software has the lowest false positive and false negative rates among all call type classifiers (26). One modification was applied. VocalMat detects only salient elements in sonograms of what was classified as "harmonic" in our previous studies (11, 12, 45) and classifies such elements (e.g., step-up and step-down) as call types. To avoid these false negative cases, we manually inspected all call types and reclassified such cases as harmonic.

UMAP. We used the UMAP method (49) to independently classify call types and evaluate the impact of *Fmr1*$^{-/y}$ and bumetanide treatment on call types. UMAP is a dimensionality reduction technique based on Riemannian geometry and algebraic topology that helps cluster data with similar features. We utilized the Python library "umap-learn" (version 0.5.5), and the quantitative parameters of VocalMat were used as inputs. The quantitative parameters included the length (duration) and bandwidth of each call, the minimum and maximum frequency values in kHz

(min_freq_main, max_freq_main, mean_freq_main, min_freq_total, max_freq_total, mean_freq_total), and sound intensity in dB (min_intens_total, max_intens_total, and mean_intens_total) of various components of each call, where "main" and "total" designate the most intense wave component and all wave components, respectively, of each call. Additionally, the following parameters were set for UMAP calculation: random_state, 0 and n_neighbors, 30. The remaining parameters were left at their default values. After call clusters were identified by UMAP, we labeled each data point based on the modified VocalMat call type classification.

To test the validity and robustness of this approach, we created bootstrapped clusters from randomly chosen data points within each call type 2000 times. Each random selection generated the median data point for each call type. These 2000 median values per call type were plotted and compared with the positions of the data point distribution of each call in UMAPs. The positions of these median values clustered at the center of each call type of UMAP, thereby validating the UMAP data.

Call Sequence Analysis. As we reported previously (11, 12), we quantitatively defined a call sequence as a series of calls with intercall intervals below the intersection between the theoretical and observed distribution curves. Two calls with an intercall interval longer than the cross-point of the two curves were considered to belong to the last and first call of two distinct call sequences. Two-call pairs within so-defined sequences were then used for Markov modeling, using our published procedure (11, 12). There were 0 counts of some call pairs in some animals. A count of 1 was added to all call pairs of each animal to avoid 0 probabilities.

Lasso Model. We applied the Lasso regression model, following our previous method (12), to extract predictive variables of the number and proportion of each call type and two-call pairs within sequences for individual social interaction scores.

Statistical Analysis

All computer programs and data are available upon request. Analysis of variance (ANOVA) was used to compare more than two groups, and Student's unpaired and paired *t*-tests were used for comparisons of two groups. The normality and homogeneity of variance of data were evaluated using the Shapiro–Wilk and Levene tests, respectively. When either assumption was violated, data were analyzed using the Mann–Whitney test for unpaired data and the Wilcoxon nonparametric test for paired data. However, when a sample size was too small for the normality test *($n < 10$)*, the homogeneity of variance alone was used to decide whether to analyze data with parametric or nonparametric tests. The minimum significance level was set at $p < 0.05$. When more than two tests were applied to a data set, the significance level was adjusted using Benjamini–Hochberg correction at a 5% false discovery rate (FDR). All statistical values are provided in Supplemental Table S2; the original *p* values that remained significant after this adjustment are shown in figure legends. Excluded cases are detailed in the *Results* section.

Study Approval

Animal handling and use followed protocols approved by the Animal Care and Use Committee of Hirosaki University Graduate School of Medicine and were in accordance with the Rules for Animal Experimentation of Hirosaki University.

Data Availability

All raw data and supporting analytical code are available upon request. All statistical data are provided in Supplemental Table S2. All reagents and the mouse model are publicly available.

Acknowledgments

We thank Ms. Sachiko Kamikawa, Mr. Daiki Tsushima, Ms. Yuriko Takagi, and Ms. Takako Takehana for technical assistance.

Author Contributions

YS conducted and designed all experiments and wrote the manuscript. TT analyzed all data, made all figures, and wrote the manuscript. SS collected data. TH analyzed all data. KN oversaw the entire work, designed all experiments, and supervised YS and SS. NH oversaw the entire analysis of all data, supervised TT and TH, analyzed all data, made figures, and wrote the entire manuscript.

The manuscript has been read and approved by all authors. All authors take full responsibility for all data, figures, and text and approve the content and submission of the study. No related work is under consideration elsewhere. All authors state that all unprocessed data are available, and all figures provide accurate presentations of the original data.

Corresponding authors: Professor Kazuhiko Nakamura for any aspect of the work except for data analyses and Professor Noboru Hiroi for data analyses. These corresponding authors take full responsibility for the submission process.

Funding Sources

The research reported in this publication was partly supported by the National Institutes of Health (R01MH099660; R01DC015776; R03HD108551; R21HD105287 to NH), the JSPS KAKENHI (JP19K17103 to YS), and the Hirosaki Institute of Neuroscience, Japan (KN). The content is solely the responsibility of the authors and does not necessarily represent the official views of the National Institutes of Health. An open-access license has been selected.

Author Disclosures

The authors have confirmed that no conflict of interest exists. The corresponding authors had full access to all the data in the study and had final responsibility for the decision to submit for publication.

References

1. Vorstman J, Sebat J, Bourque VR, Jacquemont S. Integrative genetic analysis: cornerstone of precision psychiatry. Mol Psychiatry. 2024. DOI: 10.1038/s41380-024-02706-2. PMID: 39215185
2. Li M, Shin J, Risgaard RD, Parries MJ, Wang J, Chasman D, et al. Identification of FMR1-regulated molecular networks in human neurodevelopment. Genome Res. 2020;30(3):361–74. DOI: 10.1101/gr.251405.119. PMID: 32179589; PMCID: PMC7111522
3. Leigh MJ, Hagerman RJ. Neurodevelopmental Disorders. Edited by Rubenstein JL, Rakic P, Chen B, Kwan KY, Wynshaw-Boris A. New York: Academic Press; Elsevier; 2020, chap. 15, pp. 351–75.
4. Bonaccorso CM, Spatuzza M, Di Marco B, Gloria A, Barrancotto G, Cupo A, et al. Fragile X mental retardation protein (FMRP) interacting proteins exhibit different expression patterns during development. Int J Dev Neurosci. 2015;42:15–23. DOI: 10.1016/j.ijdevneu.2015.02.004. PMID: 25681562
5. Miller JA, Ding S-L, Sunkin SM, Smith KA, Ng L, Szafer A, et al. Transcriptional landscape of the prenatal human brain. Nature. 2014;508(7495):199–206. DOI: 10.1038/nature13185. PMID: 24695229; PMCID: PMC4105188
6. Ben-Ari Y, Cherubini E. The GABA polarity shift and bumetanide treatment: making sense requires unbiased and undogmatic analysis. Cells. 2022;11(3):396. DOI: 10.3390/cells11030396. PMID: 35159205; PMCID: PMC8834580
7. Tyzio R, Cossart R, Khalilov I, Minlebaev M, Hübner CA, Represa A, et al. Maternal oxytocin triggers a transient inhibitory switch in GABA signaling in the fetal brain during delivery. Science. 2006;314(5806):1788–92. DOI: 10.1126/science.1133212. PMID: 17170309
8. Tyzio R, Nardou R, Ferrari DC, Tsintsadze T, Shahrokhi A, Eftekhari S, et al. Oxytocin-mediated GABA inhibition during delivery attenuates autism pathogenesis in rodent offspring. Science. 2014;343(6171):675–9. DOI: 10.1126/science.1247190. PMID: 24503856
9. Fuentes J, Parellada M, Georgoula C, Oliveira G, Marret S, Crutel V, et al. Bumetanide oral solution for the treatment of children and adolescents with autism spectrum disorder: results from two randomized phase III studies. Autism Res. 2023;16(10):2021–34. DOI: 10.1002/aur.3005. PMID: 37794745
10. Hiroi N. Critical reappraisal of mechanistic links of copy number variants to dimensional constructs of neuropsychiatric disorders in mouse models. Psychiatry Clin Neurosci. 2018;72(5):301–21. DOI: 10.1111/pcn.12641. PMID: 29369447; PMCID: PMC5935536
11. Takahashi T, Okabe S, Broin PÓ, Nishi A, Ye K, Beckert MV, et al. Structure and function of neonatal social communication in a genetic mouse model of autism. Mol Psychiatry. 2016;21(9):1208–14. DOI: 10.1038/mp.2015.190. PMID: 26666205; PMCID: PMC4909589
12. Nakamura M, Ye K, E Silva MB, Yamauchi T, Hoeppner DJ, Fayyazuddin A, et al. Computational identification of variables in neonatal vocalizations predictive for postpubertal social behaviors in a mouse model of 16p11.2 deletion. Mol Psychiatry. 2021;26(11):6578–88. DOI: 10.1038/s41380-021-01089-y. PMID: 33859357; PMCID: PMC8517042
13. Lai JKY, Sobala-Drozdowski M, Zhou L, Doering LC, Faure PA, Foster JA. Temporal and spectral differences in the ultrasonic vocalizations of fragile X knock out

mice during postnatal development. Behav Brain Res. 2014;259:119–30. DOI: 10.1016/j.bbr.2013.10.049. PMID: 24211451
14. Ó Broin P, Beckert MV, Takahashi T, Izumi T, Ye K, Kang G, et al. Computational analysis of neonatal mouse ultrasonic vocalization. Curr Protoc Mouse Biol. 2018;8(2):e46. DOI: 10.1002/cpmo.46. PMID: 29927553; PMCID: PMC6055925
15. Mai L, Inada H, Kimura R, Kanno K, Matsuda T, Tachibana RO, et al. Advanced paternal age diversifies individual trajectories of vocalization patterns in neonatal mice. iScience. 2022;25(8):104834. DOI: 10.1016/j.isci.2022.104834. PMID: 36039363; PMCID: PMC9418688
16. Hiramoto T, Boku S, Kang G, Abe S, E Silva MB, Tanigaki K, et al. Transcriptional regulation of neonatal neural stem cells is a determinant of social behavior. bioRxiv. 2023. https://www.biorxiv.org/content/10.1101/2021.11.12.468452v2.
17. Esposito G, Hiroi N, Scattoni ML. Cry, baby, cry: expression of distress as a biomarker and modulator in Autism spectrum disorder. Int J Neuropsychopharmacol. 2017;20(6):498–503. DOI: 10.1093/ijnp/pyx014. PMID: 28204487; PMCID: PMC5458334
18. Kikusui T, Hiroi N. A self-generated environmental factor as a potential contributor to atypical early social communication in autism. Neuropsychopharmacology. 2017;42(1):378. DOI: 10.1038/npp.2016.225. PMID: 27909329; PMCID: PMC5143512
19. Premoli M, Memo M, Bonini SA. Ultrasonic vocalizations in mice: relevance for ethologic and neurodevelopmental disorders studies. Neural Regen Res. 2021;16(6):1158–67. DOI: 10.4103/1673-5374.300340. PMID: 33269765; PMCID: PMC8224126
20. Glass TJ, Lenell C, Fisher EH, Yang Q, Connor NP. Ultrasonic vocalization phenotypes in the Ts65Dn and dp(16)1Yey mouse models of Down syndrome. Physiol Behav. 2023;271:114323.
21. Nolan SO, Hodges SL, Lugo JN. High-throughput analysis of vocalizations reveals sex-specific changes in Fmr1 mutant pups. Genes Brain Behav. 2020;19:e12611. DOI: 10.1016/j.physbeh.2023.114323. PMID: 37573959; PMCID: PMC10592033
22. Silverman JL, Yang M, Lord C, Crawley JN. Behavioural phenotyping assays for mouse models of autism. Nat Rev Neurosci. 2010;11(7):490–502. DOI: 10.1038/nrn2851. PMID: 20559336; PMCID: PMC3087436
23. Fukumitsu K, Kaneko M, Maruyama T, Yoshihara C, Huang AJ, McHugh TJ, et al. Amylin-calcitonin receptor signaling in the medial preoptic area mediates affiliative social behaviors in female mice. Nat Commun. 2022;13(1):709. DOI: 10.1038/s41467-022-28131-z. PMID: 35136064; PMCID: PMC8825811
24. Sankoorikal GMV, Kaercher KA, Boon CJ, Lee JK, Brodkin ES. A mouse model system for genetic analysis of sociability: C57BL/6J versus BALB/cJ inbred mouse strains. Biol Psychiatry. 2006;59(5):415–23. DOI: 10.1016/j.biopsych.2005.07.026. PMID: 16199013
25. Bolivar VJ, Walters SR, Phoenix JL. Assessing autism-like behavior in mice: variations in social interactions among inbred strains. Behav Brain Res. 2007;176(1):21–26. DOI: 10.1016/j.bbr.2006.09.007. PMID: 17097158; PMCID: PMC1831820
26. Fonseca AH, Santana GM, Bosque Ortiz GM, Bampi S, Dietrich MO. Analysis of ultrasonic vocalizations from mice using computer vision and machine learning. Elife. 2021;10:e59161. DOI: 10.7554/eLife.59161. PMID: 33787490; PMCID: PMC8057810
27. Reynolds CD, Nolan SO, Jefferson T, Lugo JN. Sex-specific and genotype-specific differences in vocalization development in FMR1 knockout mice. Neuroreport. 2016;27(18):1331–5. DOI: 10.1097/WNR.0000000000000701. PMID: 27824730; PMCID: PMC5290539
28. Spencer CM, Alekseyenko O, Serysheva E, Yuva-Paylor LA, Paylor R. Altered anxiety-related and social behaviors in the Fmr1 knockout mouse model of fragile X syndrome. Genes Brain Behav. 2005;4(7):420–30. DOI: 10.1111/j.1601-183X.2005.00123.x. PMID: 16176388
29. Spencer CM, Graham DF, Yuva-Paylor LA, Nelson DL, Paylor R. Social behavior in Fmr1 knockout mice carrying a human FMR1 transgene. Behav Neurosci. 2008;122(3):710–5. DOI: 10.1037/0735-7044.122.3.710. PMID: 18513141
30. Mineur YS, Huynh LX, Crusio WE. Social behavior deficits in the Fmr1 mutant mouse. Behav Brain Res. 2006;168(1):172–5. DOI: 10.1016/j.bbr.2005.11.004. PMID: 16343653
31. McNaughton CH, Moon J, Strawderman MS, Maclean KN, Evans J, Strupp BJ. Evidence for social anxiety and impaired social cognition in a mouse model of fragile X syndrome. Behav Neurosci. 2008;122(2):293–300. DOI: 10.1037/0735-7044.122.2.293. PMID: 18410169
32. Liu ZH, Smith CB. Dissociation of social and nonsocial anxiety in a mouse model of fragile X syndrome. Neurosci Lett. 2009;454(1):62–6. DOI: 10.1016/j.neulet.2009.02.066. PMID: 19429055; PMCID: PMC3092374
33. Liu Z-H, Chuang DM, Smith CB. Lithium ameliorates phenotypic deficits in a mouse model of fragile X syndrome. Int J Neuropsychopharmacolog. 2011;14(5):618–30. DOI: 10.1017/S1461145710000520. PMID: 20497624; PMCID: PMC3102293
34. Nolan SO, Reynolds CD, Smith GD, Holley AJ, Escobar B, Chandler MA, et al. Deletion of Fmr1 results in sex-specific changes in behavior. Brain Behav. 2017;7(10):e00800. DOI: 10.1002/brb3.800. PMID: 29075560; PMCID: PMC5651384
35. Roberts JE, Weisenfeld LA, Hatton DD, Heath M, Kaufmann WE. Social approach and autistic behavior in children with fragile X syndrome. J Autism Dev Disord. 2007;37(9):1748–60. DOI: 10.1007/s10803-006-0305-9. PMID: 17180715
36. Hiramoto T, Sumiyoshi A, Kato R, Yamauchi T, Takano T, Kang G, et al. Highly demarcated structural alterations in the brain and impaired social incentive learning in Tbx1 heterozygous mice. Mol Psychiatry. 2024. DOI: 10.1038/s41380-024-02797-x. PMID: 39463450
37. Kato R, Machida A, Nomoto K, Kang G, Hiramoto T, Tanigaki K, et al. Maternal approach behaviors toward neonatal calls are impaired by mother's experiences of raising pups with a risk gene variant for autism. Dev Psychobiol. 2021;63(1):108–13. DOI: 10.1002/dev.22006. PMID: 32573780; PMCID: PMC7755688
38. Kourdougli N, Nomura T, Wu MW, Heuvelmans A, Dobler Z, Contractor A, et al. The NKCC1 inhibitor bumetanide restores cortical feedforward inhibition and lessens sensory hypersensitivity in early postnatal fragile X mice. Biol Psychiatry. 2024;S0006-3223(24):01427-6. DOI: 10.1016/j.biopsych.2024.06.023. PMID: 38950809
39. He Q, Arroyo ED, Smukowski SN, Xu J, Piochon C, Savas JN, et al. Critical period inhibition of NKCC1 rectifies synapse plasticity in the somatosensory cortex and restores adult tactile response maps in fragile X mice. Mol Psychiatry. 2019;24(11):1732–47. DOI: 10.1038/s41380-018-0048-y. PMID: 29703945; PMCID: PMC6204122
40. Marlborough M, Welham A, Jones C, Reckless S, Moss J. Autism spectrum disorder in females with fragile X syndrome: a systematic review and meta-analysis of prevalence. J Neurodev Disord. 2021;13(1):28. DOI: 10.1186/s11689-021-09362-5. PMID: 34294028; PMCID: PMC8299695
41. Roy S, Watkins N, Heck D. Comprehensive analysis of ultrasonic vocalizations in a mouse model of fragile X syndrome reveals limited, call type specific deficits. PLoS One. 2012;7(9):e44816. DOI: 10.1371/journal.pone.0044816. PMID: 22984567; PMCID: PMC3439444
42. Petroni V, Subashi E, Premoli M, Wöhr M, Crusio WE, Lemaire V, et al. Autistic-like behavioral effects of prenatal stress in juvenile Fmr1 mice: the relevance of sex differences and gene-environment interactions. Sci Rep. 2022;12(1):7269. DOI: 10.1038/s41598-022-11083-1. PMID: 35508566; PMCID: PMC9068699
43. Suzuki G, Harper KM, Hiramoto T, Funke B, Lee M, Kang G, et al. Overexpression of a human chromosome 22q11.2 segment including TXNRD2, COMT and ARVCF developmentally affects incentive learning and working memory in mice. Hum Mol Genet. 2009;18(20):3914–25. DOI: 10.1093/hmg/ddp334. PMID: 19617637; PMCID: PMC2748897
44. Suzuki G, Harper KM, Hiramoto T, Sawamura T, Lee M, Kang G, et al. Sept5 deficiency exerts pleiotropic influence on affective behaviors and cognitive functions in mice. Hum Mol Genet. 2009;18(9):1652–60. DOI: 10.1093/hmg/ddp086. PMID: 19240081; PMCID: PMC2733818
45. Hiramoto T, Kang G, Suzuki G, Satoh Y, Kucherlapati R, Watanabe Y, et al. Tbx1: identification of a 22q11.2 gene as a risk factor for autism spectrum disorder in a mouse model. Hum Mol Genet. 2011;20(24):4775–85. DOI: 10.1093/hmg/ddr404. PMID: 21908517; PMCID: PMC3221538
46. Harper KM, Hiramoto T, Tanigaki K, Kang G, Suzuki G, Trimble W, et al. Alterations of social interaction through genetic and environmental manipulation of the 22q11.2 gene Sept5 in the mouse brain. Hum Mol Genet. 2012;21:3489–99. DOI: 10.1093/hmg/dds180. PMID: 22589251; PMCID: PMC3392117
47. Yamauchi T, Kang G, Hiroi N. Heterozygosity of murine Crkl does not recapitulate behavioral dimensions of human 22q11.2 hemizygosity. Genes Brain Behav. 2021;20(5):e12719. DOI: 10.1111/gbb.12719. PMID: 33269541; PMCID: PMC8169709
48. Jabarin R, Netser S, Wagner S. Beyond the three-chamber test: toward a multimodal and objective assessment of social behavior in rodents. Mol Autism. 2022;13(1):41. DOI: 10.1186/s13229-022-00521-6. PMID: 36284353; PMCID: PMC9598038
49. McInnes L, Healy J, Melville J. UMAP: Uniform manifold approximation and projection for dimension reduction. arXiv. 2018;1802.03426.